Reports

Lunar Magnetic Anomalies and Surface Optical Properties

Abstract. *For typical solar wind conditions, lunar magnetic anomalies with dipole moments* $\mathbf{m} \gg 5 \times 10^{13}$ *gauss-cubic centimeters will strongly deflect the solar wind, producing local plasma voids at the lunar surface. The correlation of the largest observed anomalies* ($\mathbf{m} \sim 10^{16}$ *gauss-cubic centimeters) with unusual, relatively high albedo surface features may therefore imply that solar wind ion bombardment is an important determinant of the optical properties of the lunar surface.*

The decoloration and darkening with time of freshly exposed surface materials, typified by the disappearance of crater rays, is a fundamental characteristic of the moon and of certain other airless planetary bodies (*1, 2*). Experimental simulations and analyses of returned lunar rock samples have established that solar wind ion bombardment (*3*) and micrometeoroid impacts (*4*) are probable contributors to the observed darkening. However, there remains little general agreement on whether one or both of the two proposed external mechanisms is dominant (*1, 5*).

In this report, we show that deflection of the solar wind by magnetic fields in regions of especially strong and coherent permanent magnetism on the lunar surface can provide a macroscopic means for distinguishing between the two general mechanisms. The largest magnetic anomaly fields are capable of at least partially shielding limited areas from the intense ion bombardment which otherwise blankets the sunward face of the moon. A comparison of measured optical properties of the shielded areas with those of unshielded areas may therefore allow an identification of properties that are dominantly solar wind-dependent. Impetus for the present report is provided by the recently discovered correlation of the largest anomalies found in Apollo subsatellite magnetometer and electron-reflectance data with the occurrence at three widely separated lunar locations of unusual, relatively high albedo surface features classified by geologists as members of the Reiner Gamma Formation (*6*). It has been shown that the anomaly sources are most probably composed of especially magnetic deposits of crater ejecta materials (*6, 6a*). We postulate here that the higher albedo and swirl-like morphology of these features are, respectively, due to deflection and focusing effects on incident solar wind ions by strong near-surface magnetic fields.

Consider a magnetic field source on the sunward face of the moon (Fig. 1). For simplicity, the uncompressed source field is assumed to be dipolar with moment $\mathbf{m}$ parallel to the lunar surface and originating at depth d. The solar wind is assumed to be normally incident on the surface with typical values of ion number density N_0 and bulk plasma velocity V_0. The nature of the interaction, including the possibility that a magnetopause boundary layer will form between the plasma and the field, is critically dependent on both the scale size and the intensity of the magnetic field (*7*). If the field is insufficiently strong or lacks coherence, the incident ions will be only slightly deflected and decelerated with a consequent mild compression of the field. This class of interaction was observed at several of the Apollo landing sites (*8*) and is undoubtedly characteristic of most of the lunar surface. If, however, in rare instances, magnetic anomalies with significantly greater strength and coherence occur, a threshold may be reached at which the anomaly field will effectively shield the surface from direct exposure to the solar wind.

In order to estimate the relevant threshold values of field strength and scale for the dipolar anomaly of Fig. 1, it is useful to consider the simpler case of planar symmetry, that is, the case in which the magnetic field extends to infinity in one direction and the plasma is incident perpendicular to the field. Exact steady-state solutions of this problem have been derived (*9*) in which the thickness, t, to the boundary layer (defined as the distance into the plasma at which the magnetic field intensity is reduced by the factor $1/e$) is given by

$$t \cong \left(\frac{m_e}{4\pi N_0}\right)^{1/2} \frac{c}{q_e} \equiv \frac{c}{\omega_p} \qquad (1)$$

where m_e and q_e are, respectively, the mass and charge of an electron; N_0 is the incident number density of either ions or electrons; c is the speed of light; and ω_p is the plasma frequency (*10*). This result is general and does not require that the surface field stand off the incident plasma; the planar boundary between the field and the plasma can just be the lunar surface. The simple dependence of the interaction on the plasma number density as expressed by Eq. 1 was consistently observed at those Apollo landing sites where significant surface magnetic fields were present (*8*).

If the field itself is responsible for establishing the planar boundary, then a pressure balance of the form

$$N_0 m_i V_0^2 = B_0^2/8\pi \qquad (2)$$

where m_i is the ion mass, V_0 is the incident bulk velocity of the plasma, and B_0 is the magnetic field strength at the boundary, must hold. Substituting for N_0 in Eq. 1 then gives an alternate expression for t,

$$t \cong \frac{(2m_e m_i)^{1/2} V_0 c}{q_e B_0} = 1.41\ a' \qquad (3)$$

where a' is defined as the geometric mean of the ion and electron Larmor radii. The effective turning radius of the incident plasma is intermediate between the electron and ion turning radii because of the existence of a polarization electric field in the boundary layer which effectively transfers momentum from the heavier ions to the electrons (*9*).

In order to stand off the solar wind and produce a local plasma void, the compressed local field must first have an amplitude sufficient to satisfy the pressure balance condition of Eq. 2. In practice, this is not a very stringent requirement since a field of only $\sim 80\ \gamma$ ($1\ \gamma = 10^{-5}$ G) will satisfy Eq. 2 for nominal solar wind parameters of 10 cm^{-3} for N_0 and 400 km/sec for V_0. Lunar surface fields of this magnitude are prevalent as evidenced by measurements exceeding 100 γ at the Apollo 14 and Apollo 16 landing sites (*11*), but, as we have emphasized, only minor deflections of the ion bombardment were observed.

The second and critical requirement is that the horizontal scale L over which the anomaly field at the boundary is essentially uniform must be much greater than the planar t value given by Eq. 1 or Eq. 3. If this requirement is not met, additional forces due to field gradients will invalidate Eq. 2 so that a higher surface field strength would be required to produce a local standoff (*7*). It should be evident that the horizontal scales of the surface magnetic fields at the Apollo landing sites are so small that Eq. 2 is not applicable.

For the dipolar field of Fig. 1, we can

0036/8075/80/0404-0049$00.50/0

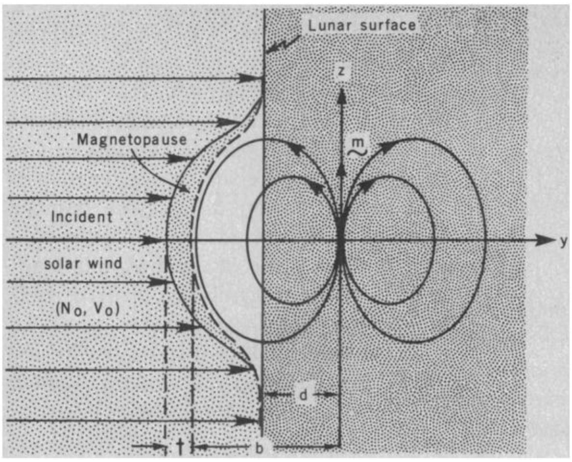

Fig. 1. Simple model for the interaction of the solar wind with a lunar crustal magnetic field represented by a buried dipole.

estimate the L over which the field is nearly uniform by taking the ratio of the parallel field intensity to the change in perpendicular field intensity with distance along the field direction. On the y-axis, $L \sim B_z/(\partial B_y/\partial z)$. Using standard formulas for the rectangular components of a dipolar field (*12*), one can evaluate this expression at the stagnation point $(0,-b,0)$ to yield $L \sim b/3$, expressing the decrease in curvature of field lines with distance from the origin. In reality, magnetopause boundary currents will reduce the curvature of the dipolar field lines near the stagnation point, and so this result may be slightly conservative.

We can further relate L to m and the solar wind parameters N_0 and V_0 by using the relation

$$N_0 m_i V_0^2 \cong \left(\frac{\frac{7}{3} m}{b^3} \right)^2 \Big/ 8\pi \qquad (4)$$

which expresses the pressure balance at the stagnation point when magnetopause boundary currents are accounted for (*13*). Thus,

$$L \sim \frac{1}{3} \left[\frac{\left(\frac{7}{3} m\right)^2}{8\pi N_0 m_i V_0^2} \right]^{1/6} \qquad (5)$$

By using Eqs. 5 and 1 and evaluating numerical constants, we find that the condition $L \gg t$ is equivalent to

$$m \gg (1.13 \times 10^7) \frac{V_0}{N_0} \qquad (6)$$

where m is units in gauss-cubic centimeters. For typical values of 10 cm^{-3} for N_0 and 400 km/sec for V_0, $m \gg 5 \times 10^{13}$ G-cm^3 is required. For rarely observed values of ~ 2 cm^{-3} for N_0 and 1000 km/sec for V_0, $m \gg 6 \times 10^{14}$ G-cm^3 is required. If, as in Fig. 1, the dipolar anomaly field originates at some depth d, then it is also required that the standoff distance b (given by Eq. 4) must be greater than d.

Let us now further consider the observational evidence. Direct measurements of lunar magnetic fields with fluxgate magnetometers on the low-orbiting Apollo subsatellites have been possible only within nearly plasma-free environments, that is, during times when the moon was in the geomagnetic tail lobes of the earth's magnetosphere or when the moon was in the solar wind but the subsatellite was in the lunar wake (*14*). These data have shown that the characteristic m values of the vast majority of lunar crustal magnetic fields fall at or below the lower limits quoted above, as expected from observations at the Apollo landing sites discussed earlier. However, in unusual cases, m values exceeding the quoted lower limits must exist to explain well-established measurements. Specifically, although weak fields are dominant across the nearside maria, a large anomaly with maximum amplitude > 20 γ at an altitude of ~ 20 km was detected with the Apollo 16 subsatellite magnetometer coincident with the unusual albedo feature Reiner Gamma (*6*) (Fig. 2, a and b). Fields with amplitude > 1 γ at an altitude of 100 km, implying surface m values of $\sim 10^{16}$ G-cm^3, were detected with the Apollo 15 subsatellite magnetometer over the Van de Graaff-Aitken region on the lunar far side. An equally intense region of strong surface magnetic fields was detected by the electron-reflectance technique across and north of Mare Marginis on the eastern limb. Both the Van de Graaff-Aitken region and the area north of Mare Marginis are marked by the occurrence of unusual swirl-like albedo features morphologically similar to those of Reiner Gamma and classified geologically as members of the Reiner Gamma Formation (*15*).

Observations of increased magnetic field fluctuations in the solar wind upstream from the moon when the Apollo 15 subsatellite was over the Reiner Gamma feature and over the area north of Mare Marginis have recently been reported by Weiss (*16*). These observations are consistent with the possibility that a relatively strong interaction of solar wind plasma with local magnetic fields occurs in these regions.

It is of interest to utilize the low-altitude Apollo 16 subsatellite magnetometer measurements to estimate the surface area that would be largely shielded from the solar wind by the Reiner Gamma anomaly. For this purpose, we have applied a minimum-variance criterion to select the source depth, orientation, and m value of a simple dipole which most closely reproduces the Reiner Gamma anomaly field according to available measurements. The final model source parameters (root-mean-square 2.6 γ) include an m value of 1.9×10^{16} G-cm^3, a source depth of 32 km, and an inclination to the lunar surface of 30°. Since m is of the order of 10^{16} G-cm^3, we will assume (according to Eq. 6) that a magnetopause

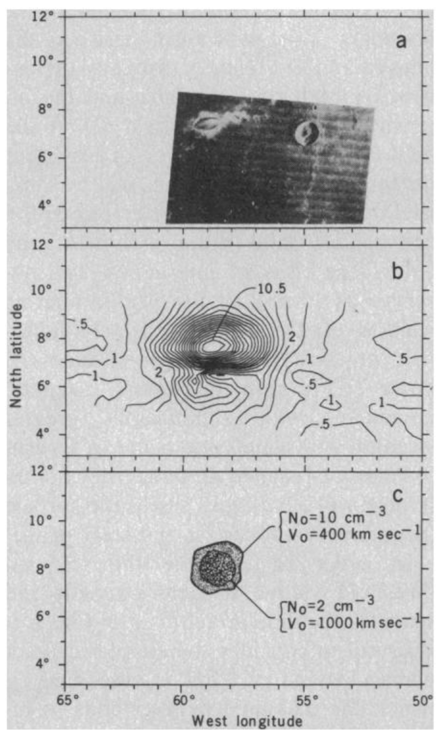

Fig. 2. (a) Lunar Orbiter 4 frame 157 oriented with respect to a longitude-latitude grid. The crater Reiner is at right, and the albedo feature Reiner Gamma is at the center. (b) Contour map of the total magnetic field intensity (in gammas) based on available orbit segments. The data have been smoothed two-dimensionally so that the total amplitude shown is less than that on single orbit plots. (c) Area of the surface that would be shielded from direct bombardment by the solar wind by a buried dipole representing the Reiner Gamma magnetic field. The light shaded area is for nominal solar wind conditions; the dark shaded area is for maximum solar wind pressures.

current system will be set up analogous to but much smaller than that which characterizes a planetary magnetosphere. One approach toward estimating the shielded area is simply to calculate the intersection of the lunar surface with a hypothetical magnetosphere that would be produced by the model dipole. From Eq. 4, using $N_0 = 10$ cm^{-3}, $V_0 = 400$ km/sec, and $m = 2 \times 10^{16}$ G-cm^3, we find $b \cong 44$ km; this result implies that the stagnation point is roughly 12 km above the lunar surface. For comparison, $t = 1.7$ km for the same parameters. To find the surface area subtended by the magnetosphere, we take into account the tilt of the dipole by interpolation from the numerically derived surfaces of Choe *et al.* (*17*). The result is shown by the light shaded area of Fig. 2c. For the extreme values of $N_0 = 2$ cm^{-3} and $V_0 = 1000$ km/sec, we find $b \cong 36.5$ km; this value implies a more marginal standoff height of ~ 4.5 km with $t \cong 3.8$ km (dark shaded area of Fig. 2c).

Of course, the actual source of the Reiner Gamma anomaly is more probably a complex distribution of near-surface magnetization rather than a buried dipole (*6*). Higher order moments will affect both the magnetospheric surface shape and the compression of the field by varying solar wind conditions. We should therefore expect a more complex shape for the shielded region than that indicated in Fig. 2c. Strong field inhomogeneities near the surface would tend to focus and scatter incident charged particles, producing a spatially variable surface flux distribution. If the surface ion flux is a dominant determinant of surface optical properties, then an unusual albedo pattern, not unlike the swirl-like morphology of the Reiner Gamma Formation, would be produced.

L. L. HOOD
Lunar and Planetary Laboratory, University of Arizona, Tucson 85721

G. SCHUBERT
Department of Earth and Space Sciences, University of California, Los Angeles 90024

References and Notes

1. D. Matson, T. Johnson, G. Veeder, *Proc. 8th Lunar Sci. Conf.* (1977), p. 1001.
2. B. Hapke, in *Physics and Astronomy of the Moon*, Z. Kopal, Ed. (Academic Press, New York, ed. 2, 1971), p. 155; T. McCord and J. Adams, *Moon* **7**, 453 (1973).
3. Darkening of silicate rock powders by formation of hydrogen ion-sputtered glass films containing iron and titanium has been simulated in the laboratory by B. Hapke [*Moon* **7**, 342 (1973)]. A similar experiment in which the albedo of a pulverized Apollo rock sample was lowered was interpreted as due to an increase in the surface concentrations of iron and titanium by direct sputter reduction [T. Gold, E. Bilson, R. Baron, *Proc. 7th Lunar Sci. Conf.* (1976), p. 901]. Reports of other relevant experiments are discussed in the references of these papers.
4. Production of dark glass fragments by meteoroid and micrometeoroid impacts has been experimentally investigated as a possible mechanism for reducing the albedo of lunar soils by D. B. Nash, J. E. Conel, and R. T. Greer [*Science* **167**, 721 (1970)] and J. Conel and D. Nash [*Proc. Apollo 11 Lunar Sci. Conf.* (1970), p. 2013]. Differences between spectral reflectance curves for Apollo 11 and Apollo 12 soil samples were interpreted as due to variations in the amounts of impact-generated dark glass present in the soils [J. B. Adams and T. B. McCord, *Science* **171**, 567 (1971)].
5. Vapor deposits produced by solar wind sputtering or micrometeoroid impacts, or both, are considered to be the main determinant of the optical properties of the lunar surface [B. Hapke, W. Cassidy, E. Wells, *Moon* **13**, 339 (1975); E. Wells and B. Hapke, *Science* **195**, 977 (1977)]. Both solar wind exposure and agglutinate formation during micrometeoroid impacts are likely contributors to the darkening process according to R. Housley [*Philos. Trans. R. Soc. London Ser. A* **285**, 363 (1977)]. A coherent summary of the several proposed darkening mechanisms has been presented by L. Yin, T. Tsang, and I. Adler [*Geophys. Res. Lett.* **2**, 33 (1975)].
6. L. L. Hood, P. J. Coleman, Jr., D. E. Wilhelms, *Science* **204**, 53 (1979); *Proc. 10th Lunar Planet. Sci. Conf.*, in press.
6a. D. Strangway, W. Gose, G. Pearce, R. M. McConnell, *Nature (London)* **246**, 112 (1973).
7. A. Barnes, P. Cassen, J. D. Mihalov, A. Eviatar, *Science* **172**, 716 (1971); G. Siscoe and B. Goldstein, *J. Geophys. Res.* **78**, 6741 (1973).
8. P. Dyal, C. Parkin, C. Snyder, D. Clay, *Nature (London)* **236**, 381 (1972); D. Clay, B. Goldstein, M. Neugebauer, C. Snyder, *J. Geophys. Res.* **80**, 1751 (1975); L. Vanyan, *Moon* **16**, 321 (1977); P. Dyal, W. Daily, L. Vanyan, *Proc. 9th Lunar Planet. Sci. Conf.* (1978), p. 231.
9. C. Longmire, *Elementary Plasma Physics* (Interscience, New York, 1963), p. 90.
10. Gaussian units are used throughout this report.
11. P. Dyal, C. Parkin, W. Daily, *Rev. Geophys. Space Phys.* **12**, 568 (1974).
12. H. Alfvén and C. Fälthammar, *Cosmical Electrodynamics* (Oxford Univ. Press, London, 1963), p. 5.
13. G. Mead, *J. Geophys. Res.* **69**, 1181 (1964).
14. L. Hood, P. Coleman, Jr., C. Russell, D. Wilhelms, *Phys. Earth Planet Inter.* **20**, 291 (1979).
15. F. El-Baz, *NASA Spec. Publ. SP-315* (1972), p. 29:93; P. Schultz, *Moon Morphology* (Univ. of Texas Press, Austin, 1976), pp. 420–423.
16. H. Weiss, thesis, University of California, Los Angeles (1979), pp. 42–45.
17. J. Choe, D. Beard, E. Sullivan, *Planet. Space Sci.* **21**, 285 (1973).
18. We are grateful to F. Herbert for our initial interest in this problem and to C. T. Russell for enlightening criticisms. Useful discussions with C. P. Sonnett, P. J. Coleman, Jr., and D. E. Wilhelms are also acknowledged. Supported under NASA grants NSG 7020 (at the University of Arizona) and NSG 7315 (at the University of California, Los Angeles).

28 September 1979; revised 26 December 1979

Is the Sun Shrinking?

Abstract. *Observations of 23 transits of Mercury in front of the sun between 1736 and 1973 show no indication of any significant change in the diameter of the sun. Regression analysis yields a decrease of the angular diameter, as viewed from the earth, of under 0.3 arc second per century (> 90 percent confidence limit). This limit is incompatible with the 2 arc seconds per century decrease obtained by Eddy for the equatorial diameter from direct observations made at the Greenwich Observatory and at the U.S. Naval Observatory.*

Recently, Eddy (*1*) reported that the diameter of the sun, as viewed from the earth, may be decreasing at the strikingly large rate of about 2 arc seconds per century. This rate can clearly not be constant; if it were, the sun would shrink to a point in 100,000 years and would have been twice its present diameter 100,000 years ago. If, instead, this rate were periodic, with a period of centuries, its importance to our understanding of the sun would be great. I therefore sought corroborative evidence of a change in the diameter from an analysis of observations of the transits of the planet Mercury in front of the sun. These astronomical events take place about 13 times per century; they occur only in May and November, when the earth and Mercury are nearly aligned, on the same side of the sun, along the intersection of their orbital planes. Such transits have been observed regularly, with small telescopes, since the late 17th century. Traditionally, the times of up to four individual events have been recorded for each transit: the successive apparent external and internal contacts, or osculations, of the disks of Mercury and the sun (see Fig. 1). Until 30 years ago, the clocks used to time these events were based on the rotation of the earth. Because these observations consist only of the times of contact, they are virtually free from dependence on all the other variables, such as star positions, that often plague astronomical observations and their interpretation. This advantage is partially offset by the difficulty of accurately determining the instants of contact (*2*), a problem less severe for the internal contacts.

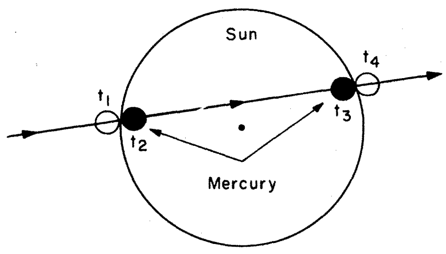

Fig. 1. Sketch of the view from the earth as Mercury transits in front of the solar disk. The observations consist of the times of external contact, t_1 and t_4, and internal contact, t_2 and t_3 ($t_1 < t_2 < t_3 < t_4$).

Primarily because of their extreme importance for the experimental foundation of the law of gravitation, the transit data

0036/8075/80/0404-0051$00.50/0